

NACA RM E9K17

E9K17

**NACA**

0143657

TECH LIBRARY KAFB, NM

# RESEARCH MEMORANDUM

TURBOJET-ENGINE EVALUATION OF AISI 321 AND AISI 347

STAINLESS STEELS AS NOZZLE-BLADE MATERIALS

By Floyd B. Garrett and Charles Yaker

Lewis Flight Propulsion Laboratory  
Cleveland, Ohio

**AFMDC  
TECHNICAL LIBRARY  
AFL 2811**



**NATIONAL ADVISORY COMMITTEE  
FOR AERONAUTICS**

WASHINGTON  
February 27, 1950

6889

219.94/13



## NATIONAL ADVISORY COMMITTEE FOR AERONAUTICS

RESEARCH MEMORANDUM

## TURBOJET-ENGINE EVALUATION OF AISI 321 AND AISI 347

## STAINLESS STEELS AS NOZZLE-BLADE MATERIALS

By Floyd B. Garrett and Charles Yaker

## SUMMARY

An investigation was conducted to evaluate the engine service performance of nozzle-diaphragm blades of AISI 321 (titanium modified) and of AISI 347 (columbium modified) stainless steels. Data were obtained from three nozzle diaphragms alternately bladed with each of the two materials. In order to simulate conditions of normal service, the nozzle diaphragms were subjected to 20-minute cycles of engine operation consisting of 5 minutes at idle and 15 minutes at rated speed.

Cracks started as early as 80 cycles (26 hr, 40 min) in one diaphragm and as late as 240 cycles (80 hr) in another. After one diaphragm had been operated 319 cycles (106 hr, 20 min), 21 of 24 AISI 321 blades and 19 of 24 AISI 347 blades were cracked, but in no case did a complete rupture occur. The blade cracks, which occurred principally in the edges of the blades, were attributed to thermal stresses and to oxidation by the turbine gas. The cracks progressed through the material along the grain boundaries. Cracks were also observed in unsound zones of scale in the welds of both alloys on the inner-spacer ring after 80 hours of operation.

## INTRODUCTION

Stainless steels of the 18-percent chromium, 8-percent nickel type have desirable high-temperature properties. One of the disadvantages of these stainless steels, however, is susceptibility to intergranular corrosion after exposure to the temperature range between 750° and 1650° F (reference 1). The formation at these temperatures of a carbide in the grain boundaries of the steel is responsible for the poor resistance to intergranular corrosion. The formation of grain-boundary carbides can be reduced by (1) lowering the carbon content of the steel to the solubility limit of the alloy, or (2) stabilizing the steel to reduce the carbon

available for precipitation. The first method is self-explanatory; the second method consists in adding elements that have strong carbide-forming tendencies and will, with the proper heat treatment, form carbides that precipitate in the matrix of the steel. This precipitation reduces the free-carbon content of the matrix and reduces the formation of intergranular carbides. The stabilization method is more practicable because of the high cost of producing low-carbon stainless steel.

Titanium and columbium are the elements most commonly used as stabilizers of stainless steel. Investigators have determined that a certain minimum ratio of stabilizing element to carbon is necessary to prevent intergranular corrosion (reference 2). The data in reference 2 indicate that for stainless steel with a ratio of columbium to carbon of 10 or a ratio of titanium to carbon of 5 an annealing treatment and air-cooling will produce a stabilized material.

Columbium has been widely used in preference to titanium as a stabilizing element because of the greater ease of welding during fabrication. Columbium, however, is a critical alloying material and was considered as insufficient in supply for industrial use in 1944 (reference 3); whereas titanium is readily available, and therefore more desirable.

As part of a general evaluation of various heat-resisting alloys for jet-engine and gas-turbine applications, investigations were conducted at the NACA Lewis laboratory on three turbine-nozzle diaphragms fabricated with alternate blades of AISI 321 and of AISI 347 stainless steel to compare the performance of the two steels under service conditions. The AISI 347 stainless steel was in use as a blade material at the time this investigation was conducted. Both steels contain approximately 18-percent chromium and 10-percent nickel. The AISI 321 and the AISI 347 steels are stabilized with titanium and columbium, respectively. In order to avoid the difficult welding techniques necessary with titanium-stabilized rods, the AISI 321 blades were welded with molybdenum steel welding rods containing 19-percent chromium and 9-percent nickel. The AISI 347 blades were welded with AISI 347 welding rods.

A cyclic-type engine operation was chosen to simulate the starting and shutdown conditions in service operation. Each nozzle diaphragm was subjected to the same cyclic conditions. After completing the cyclic engine operation, the nozzle diaphragms were metallurgically examined in an attempt to identify the mechanisms of failure.

## APPARATUS AND PROCEDURE

## Nozzle Diaphragms

Cyclic engine evaluation was made of three nozzle diaphragms having odd numbered blades of AISI 321 stainless steel and even numbered blades of AISI 347 stainless steel. The downstream face of a diaphragm before operation is shown in figure 1.

Chemical composition. - The chemical analyses of the nozzle blades are presented in table I. Three analyses are listed for the AISI 347 steel as there were three lots of material in the fabrication shop at the time the diaphragms were made. Some blades in each diaphragm may be of each lot. All AISI 321 blades were from one lot of the analysis presented in table I.

Fabrication. - The nozzles were forged using standard procedures. The parts were annealed for 45 minutes after forging, the AISI 321 blades at 1900° F and the AISI 347 blades at 1950° F, followed by air-cooling.

For all diaphragms, the outer- and inner-spacer rings, diaphragm-baffle assembly, and inner-diaphragm ring were made of AISI 347 steel.

After the parts were welded into an assembly, the full assembly was slowly heated to 1100° F, annealed at 1950° F for 30 minutes, and air-cooled.

## Engine Setup

The investigation of the three nozzle diaphragms was conducted on several turbojet engines mounted in a pendulum-type sea-level test stand. The engines, having a sea-level static thrust rating of approximately 4000 pounds, incorporated a dual-entry centrifugal compressor, 14 combustion chambers, and a single-stage turbine.

Gas temperature was measured at the exhaust-cone outlet by 14 unshielded chromel-alumel thermocouples equally spaced about the circumference and radially extending 2 inches into the tail pipe. Gas temperature at the exhaust-cone outlet was controlled by a variable-area jet nozzle. The fuel used was AN-F-32.

### Engine Operation

For each run, an engine was assembled with one of the three special nozzle diaphragms. The engine was operated at a rotor speed of 6000 rpm to check the condition of the engine before starting the cyclic runs each day. After the engine check was made, the engine was subjected to 20-minute cycles of operation. The sequence of operation, comprising one cycle, is outlined in the following table:

Duration (min) (sec)		Rotor speed (rpm)	Gas temperature at exhaust-cone outlet (°F)
4	30	4000 ± 50	1110 maximum
0	15	Acceleration to 11,500	1450 ± 50
15	0	11,500 ± 50	1240 ± 20
0	15	Deceleration to 4000	1260 maximum

Visual-inspection procedures were followed in examining the nozzle blades during engine shutdown and overhaul periods. The diaphragms were operated until severe cracking of the blades occurred or until other factors, such as warpage, prevented satisfactory engine operation.

### Metallurgical Examination

After the engine runs were completed, standard metallurgical procedures were used to examine the nozzle blades. All nozzle blades and welds were examined without magnification or under a low-power microscope to determine surface condition and oxide coloring and a fluorescent-oil examination was used to determine the number and the location of cracks in the blades and the welds. Microexamination of several cracked and uncracked blades of both types of material was used to determine grain size, precipitation characteristics, and the nature of crack propagation. All specimens were electrolytically etched using a 10-percent solution of aqueous oxalic acid.

### RESULTS AND DISCUSSION

The results are discussed in the following paragraphs with respect to visual inspection and metallurgical examination.

## Visual Inspection

1212

Nozzle diaphragm 1. - Nozzle diaphragm 1 was operated for a total of 240 cycles (80 hr), after which the runs were terminated because of the presence of large cracks in the blades and damage caused by failure of other engine components.

Nozzle diaphragm 2. - After 80 cycles (26 hr, 40 min) of operation, runs on nozzle diaphragm 2 were concluded because of warpage of the outer-spacer ring caused by insufficient support by the tail cone while operating in the engine.

Nozzle diaphragm 3. - Nozzle diaphragm 3 was operated for 319 cycles (106 hr, 20 min). Operation was concluded at this time because of the formation of very large cracks in many of the blades.

The results of the visual inspections of the three nozzle diaphragms are summarized in table II. The visual inspections showed that cracking started in nozzle diaphragm 1 between 176 cycles (58 hr, 40 min) and 240 cycles (80 hr), and in nozzle diaphragm 3 between 100 cycles (33 hr, 20 min) and 110 cycles (36 hr, 40 min). No cracking was evident in nozzle diaphragm 2 after 80 cycles (26 hr, 40 min).

Examination of the nozzle diaphragms after operation revealed that a definite relation exists between burner location and blade cracks. Typical examples of the condition of the diaphragm blades after 319 cycles (106 hr, 20 min) of operation are shown in figure 2. These photographs clearly indicate that the severely cracked blades are generally located opposite the center of the burner outlet. Slight differences were noted between blades opposite various burners, which can be attributed to differences in combustion characteristics of the burners.

Examination of the cracked blades for warpage showed the leading edges to be straight. Some of the trailing edges were warped into several waves, although others were straight.

Although cracks started between 100 and 110 cycles (approximately 33 and 37 hr) of operation of nozzle diaphragm 3 and increased in number and size up to about 319 cycles (106 hr) of operation, none of the nozzle blades completely broke.

## Metallurgical Examination

The following results were obtained from the metallurgical examination of the three nozzle diaphragms:

All nozzle blades were covered with a dark blue-gray oxide. Slight surface pitting was evident on the faces of both AISI 321 and AISI 347 nozzle blades. The pits were shallow and no measurable difference in amount of pitting of the two alloys existed.

Fluorescent-oil inspection. - Results of the fluorescent-oil inspection of the three nozzle diaphragms are given in table III. The results for the two different alloys are summarized in the following table:

	Nozzle diaphragm 1 after 240 cycles (80 hr)		Nozzle diaphragm 2 after 80 cycles (26 hr, 40 min)		Nozzle diaphragm 3 after 319 cycles (106 hr, 20 min)	
	AISI 321	AISI 347	AISI 321	AISI 347	AISI 321	AISI 347
Number of cracked blades	14	16	0	1	21	19
Total number of cracks	62	99	0	3	208	218

After 319 cycles (106 hr, 20 min) of engine operation, 21 of 24 AISI 321 blades were cracked with a total of 208 cracks, and 19 of 24 AISI 347 blades were cracked with a total of 218 cracks. In no case did the cracking cause a complete rupture of any portion of the blades. These results indicate that cracking started about cycle 80 (26 hr, 40 min) in nozzle diaphragm 2, which was early in comparison with the other two nozzle diaphragms. This early occurrence of cracking indicated that visual inspection during engine shutdown was not too critical, inasmuch as no cracks were noted in this diaphragm until the diaphragm was removed from the engine. On the basis of performance in an engine, no difference exists between the two alloys in resistance to cracking. The number of cracks in the blades is an incomplete measure of crack resistance, inasmuch as crack depth was not included. In general, it was observed, however, that the crack depth in both types of blade was of the same order of magnitude. Cracks in the leading edges were as much as  $1/2$  inch long, whereas those in the trailing edges were as much as  $1\frac{1}{2}$  inches long.

The trailing edges contained considerably fewer cracks than the leading edges, as shown in table III. Figure 3 is typical of the cracking observed in both types of blade. The difference in the number of cracks between the leading and trailing edges is apparent in this figure.

Because of the nature of construction of the nozzle diaphragms, no inspection of the welds could be made during operation. Fluorescent-oil inspection at the conclusion of operation gave the following results:

(1) Nozzle diaphragm 1 had no cracked welds after 240 cycles (80 hr) of operation.

(2) Nozzle diaphragm 2 had no cracked welds after 80 cycles (26 hr, 40 min) of operation.

(3) Nozzle diaphragm 3 had ten cracked welds in the AISI 321 blades and eight in the AISI 347 blades after 319 cycles (106 hr, 20 min) of operation. All cracks were on the inner-spacer ring of the diaphragm.

One of the more severe weld cracks is shown in figure 4. The location of the crack is typical of both types of weld. Shown also is a crack in the spacer ring at the end of the expansion slot. Cracks of this type were found at the end of all the expansion slots in the inner-spacer ring of nozzle diaphragm 3. Similar cracks were present in nozzle diaphragm 1 but not in nozzle diaphragm 2.

Microexamination. - Grain-size measurements showed that all nozzle blades of each alloy were of approximately the same grain size and that all were generally finer grained at the leading and trailing edges than in the center. The AISI 321 nozzle blades had an A.S.T.M. grain size between 5 and 6 and the AISI 347 blades had an A.S.T.M. grain size between 6 and 7.

The structures of the two types of alloy before operation are shown in figure 5. Each structure consisted of small equiaxed grains of austenite containing small patches of complex carbides. Typical leading-edge cracks in the two alloys after 319 cycles (106 hr, 20 min) are shown in figure 6. This figure indicates that some intergranular penetration and precipitation have occurred at the leading edge of the AISI 347 blade. The AISI 321 blade shows no appreciable intergranular penetration. Each of the cracks shown is about 1/32 inch long. In the case of both blades, there were much longer cracks; and in the case of AISI 347 blades, the cracks

extended far beyond the area of intergranular penetration. A typical trailing-edge crack is shown in figure 7. This crack is representative of trailing-edge cracks in both types of alloy. In neither alloy did appreciable intergranular penetration of the trailing edge occur. The alloy structure along the crack (fig. 7(b)) shows evidence of a heavy intergranular precipitate. This precipitate was visible in the trailing edges of both types of blade and in the leading edge of the AISI 347 blades. Inasmuch as some blades were warped at the trailing edge, the edges were evidently highly stressed. The presence of large stresses probably increased the rate of precipitation in the grain boundaries near the trailing edge.

The nature of the crack propagation could not be determined in many cases because oxidation occurred along the crack surfaces during operation subsequent to cracking. The cracks in both the leading and trailing edges of both alloys generally progressed in a direction normal to the edge.

Examination of the cracked AISI 347 blade in nozzle diaphragm 2 indicated that the cracks in both the leading and trailing edges were intergranular. These cracks contained little or no oxide, inasmuch as they occurred between 70 (23 hr, 20 min) and 80 cycles (26 hr, 46 min) of operation with no further operation. The intergranular penetration at the tip of a crack, which is typical of cracks in both edges, is shown in figure 8. Two types of penetration beginning at the leading edge of a blade are indicated in figure 9. One type is intergranular penetration, and the other is surface pitting.

Examination of the weld cracks of both blade alloys indicated evidence of welding scale in the cracks (fig. 10).

#### Mechanism of Cracking

Thermal stresses. - In the cyclic engine operation there is a sudden acceleration from 4000 rpm at a temperature of  $1110^{\circ}\text{F}$  (duration, 15 sec; gas temperature,  $1450 \pm 50^{\circ}\text{F}$ ), followed by steady-state operation (duration, 15 min, gas temperature,  $1240 \pm 20^{\circ}\text{F}$ ), and then rapid deceleration. These three operating phases produce various temperature states in the nozzle blades.

During the steady-state operation, the nozzle blades are subjected to stresses that are caused by temperature differences due

to the burner location. The hotter blades have a tendency to stretch more than the cooler blades. These conditions result in a steady-stress state existing in the blades.

While accelerating and decelerating, very rapid heating and cooling of the blades occurs, respectively. When rapid heating of a nozzle blade occurs, a zone on the leading edge and a zone on the trailing edge suddenly become hot, whereas most of the blade is still cold. The hot zones tend to expand, but the cold portion of the blade resists this expansion and compressive stresses are set up in the edges. The stresses in the trailing edge are, in some cases, great enough to cause plastic flow and subsequent warping because of the very small cross section of the trailing edge. When the edge warps, the fibers on the convex side are in tension and those on the concave side are in compression. On rapid cooling, the zones along the trailing and leading edges suddenly become cool. These zones tend to contract; however, the large portion of the blade, which is still hot, resists the contraction. This resistance sets up tensile stresses in the leading and trailing edges. In the warped trailing edges, the tensile stress in the outer fibers becomes very large because of the added tensile stress produced by cooling and the inner-fiber stress reverses from compression to tension. These stresses may be of sufficient magnitude to cause cracking.

Oxidizing atmosphere. - Another possible cause of failure is the highly oxidizing atmosphere in the engine. The nozzle blades are therefore subjected to the combined effects of an oxidizing atmosphere and constant and alternating stresses during cyclic operation. Conditions are thus obtained that are favorable for stress and corrosion-fatigue failure. Corrosion fatigue requires a corrosive atmosphere and alternating stresses. The presence of the fatigue stresses causes a rapid acceleration in the crack penetration of a material even though the stresses are small.

Corrosion fatigue. - The nature of the corrosion-fatigue-failure mechanism is described in reference 4. The cracks described are similar to those observed in the leading edge of the nozzle blades (fig. 3). Corrosion-fatigue cracks form in the following manner (reference 4):

(a) Surface pits filled with an oxide scale form as the result of normal corrosion. The base of each pit is anodic to the material surface.

(b) The alternating stresses cause a concentration of stress at the base of the corrosion pit and also rupture the oxide scale, exposing the metallic surface to the corrosive atmosphere.

(c) The exposed metal, which is highly stressed, rapidly corrodes and the crack penetrates directly into the metal. This process continues until the crack penetrates to a depth where the electromotive force of the corrosion cell between the surface and the crack tip is less than that between the surface and the base of another surface pit. At this point, another surface pit starts corroding into the material. This mechanism occurs all along the edge, resulting in a series of cracks of various depths.

### Classification of Failures

Leading edge. - Microexamination indicated that the leading-edge cracks of the two alloys (fig. 6) were different in nature. The AISI 347 blade cracks were similar to an intergranular creep type of failure and the AISI 321 blade cracks similar to corrosion-fatigue failure. The AISI 321 blades also revealed some intergranular cracks (fig. 9). In both cases, however, the number of cracks and their respective depths were of the same magnitude. The exact mechanism of cracking cannot be determined, but these failures can be regarded as resulting from the combined effects of constant thermal stress, alternating sudden thermal stress, and the oxidizing atmosphere.

Trailing edge. - The cracks in the trailing edges are different from those in the leading edges. Instead of exhibiting a large number of cracks, as evidenced in the leading edge, there were only a few large cracks. Microexamination indicated a crack propagation similar to that produced by corrosion fatigue. Evidence of intergranular cracking, however, was also present. Because many of the blades had warped trailing edges, it is apparent that the thermal stresses were higher in the trailing edge than in the leading edge. This increase is due to the thinness of the trailing edge. These cracks may therefore result from stress only. Once cracks started, successive cycles resulted in deeper cracking, relieving the stress and leaving the rest of the edge crack free.

Failure of welds and inner-spacer ring. - The weld and inner-spacer-ring-slot cracks were probably caused by stresses resulting from unequal thermal expansion between blades due to differences in temperature between burner centers and edges and also differences in temperature from burner to burner. These conditions can possibly be eliminated by changes in design.

High-temperature corrosion. - Corrosion at elevated temperatures presents a very complex problem. The resistance of stainless-steel alloys to intergranular corrosion has been established by many

investigators, who employed the following procedure to evaluate the alloys: (1) stabilization by heat treatment, (2) heating the alloys to a temperature that produces susceptibility to intergranular corrosion (750° to 1650° F), and (3) measuring the intergranular-corrosion penetration by a standard procedure. The standard procedures for determining the quantity of intergranular penetration are usually performed in a corrosive liquid at a temperature approximately the boiling point of water. On the basis of these procedures, the alloys used in this investigation with the heat treatments employed are not susceptible to intergranular corrosion. When used as nozzle blades, however, these alloys must perform at elevated temperatures under thermal stress and an oxidizing atmosphere. These conditions resulted in intergranular cracking of steels considered unsusceptible to intergranular corrosion, which suggests that the laboratory procedures based on intergranular corrosion resistance alone are unsatisfactory for high-temperature alloys for uses, such as nozzle blades, and should be modified to give data that would apply to service conditions.

#### SUMMARY OF RESULTS

A cyclic engine evaluation of three nozzle diaphragms with alternate turbine-nozzle blades of AISI 321 (titanium modified) and AISI 347 (columbium modified) stainless steel was conducted and the following results were obtained:

1. Initial cracks formed in the blades as early as 80 cycles (26 hr, 40 min) of engine operation in one nozzle diaphragm and as late as 240 cycles (80 hr) of engine operation in another nozzle diaphragm.

2. After 319 cycles (106 hr, 20 min) of engine operation, 21 of 24 AISI 321 blades were cracked, with a total of 208 cracks, and 19 of 24 AISI 347 blades were cracked, with a total of 218 cracks. In no case did the cracking cause a complete rupture of any portion of the blades.

3. After about 80 hours of operation, no weld of either type of blade was cracked. After about 319 cycles (106 hr) of engine operation, ten welds of the AISI 321 blade welded with molybdenum steel welding rods containing 19-percent chromium and 9-percent nickel were cracked, and eight welds of the AISI 347 blade welded with AISI 347 rods were cracked. All weld cracks were in the inner-spacer ring of the nozzle diaphragm.

4. Cracks were found at the end of all the inner-spacer-ring slots in nozzle diaphragms 1 and 3 after 240 cycles (80 hr) and 319 cycles (106 hr, 20 min) of engine operation, respectively. No cracks were found in the inner-spacer-ring slots of nozzle diaphragm 2 after 80 cycles (26 hr, 40 min) of engine operation.

5. Cracking in the leading and trailing edges of both types of blade was attributed to the combined effects of thermal stress and the oxidizing atmosphere in the gas turbine. The cracks progressed through the materials along the grain boundaries.

6. Weld cracks of both alloys apparently occurred only in zones containing welding scale.

#### CONCLUSION

No significant difference in engine performance based on resistance to cracking exists between nozzle blades of AISI 321 (titanium stabilized) and of AISI 347 (columbium stabilized) stainless steels.

Lewis Flight Propulsion Laboratory,  
National Advisory Committee for Aeronautics,  
Cleveland, Ohio.

#### REFERENCES

1. Binder, W. O.: The Resistance of Wrought Stainless Steels to Corrosion. Metals Handbook, 1948 Edition. Am. Soc. Metals (Cleveland), 1948, pp. 557-562.
2. Rosenberg, Samuel J., and Darr, John H.: Stabilization of Austenitic Stainless Steel. Trans. A.S.M., vol. 41, 1949, pp. 1261-1288; discussion, pp. 1288-1300.
3. DeMille, John B.: Strategic Minerals. McGraw-Hill Book Co., Inc., 1947, pp. 134-137.
4. Evans, Ulick R.: Metallic Corrosion, Passivity and Protection. Longmans, Green & Co., Inc., 2d ed., 1946, pp. 437-442.

TABLE I - CHEMICAL COMPOSITION OF AISI 321 AND AISI 347  
STAINLESS STEELS

Composition	AISI 321	AISI 347		
		Lot 1	Lot 2	Lot 3
Carbon, C	0.08	0.067	0.086	0.066
Manganese, Mn	.60	1.26	1.25	1.35
Phosphorous, P	.062	.023	.020	.024
Sulfur, S	.015	.013	.019	.010
Silicon, Si	.66	.47	.61	.40
Nickel, Ni	9.57	10.12	10.18	10.13
Chromium, Cr	19.10	17.55	17.55	17.42
Titanium, Ti	.45	-----	-----	-----
Columbium, Cb	-----	.77	.78	.80
Copper, Cu	-----	.08	.08	.15
Iron, Fe	Balance	Balance	Balance	Balance
Titanium-carbon ratio, Ti/C	5.62	-----	-----	-----
Columbium-carbon ratio, Cb/C	-----	11.5	9.07	12.12



TABLE II - SUMMARY OF VISUAL INSPECTIONS DURING ENGINE SHUTDOWN PERIODS

Nozzle diaphragm 1			Nozzle diaphragm 2			Nozzle diaphragm 3		
Duration		Condition	Duration		Condition	Duration		Condition
Cycles	(hr) (min)		Cycles	(hr) (min)		Cycles	(hr) (min)	
20 <sup>a</sup>	6 40	No visible cracking.	15 <sup>a</sup>	5	No visible cracking.	25 <sup>a</sup>	8 20	No visible cracking.
45	15	Five blades dented in leading edge because of burner-strap failure.	25	8 20	Turbine-blade failure caused slight trailing-edge damage.	50	16 40	No change.
65 <sup>a</sup>	21 40	No cracks or further damage visible.	35 <sup>a</sup>	11 40	No change.	75	25	No change.
85	28 20	Trailing edges damaged by turbine-blade failure.	70 <sup>a</sup>	23 20	No change.	100 <sup>a</sup>	33 20	No change.
110 <sup>a</sup>	36 40	No cracks or additional damage visible.	80	26 40	Inspection revealed diaphragm warpage due to insufficient support. Evaluation was concluded because of warpage.	110	36 40	Three blades had small trailing-edge cracks.
176 <sup>a</sup>	58 40	No change in condition.				135	45	Six blades had small trailing-edge cracks.
240	80	Cracking of blades started. Evaluation concluded because of cracks and previous damage.				319	106 20	Evaluation concluded because of badly cracked condition of blades.

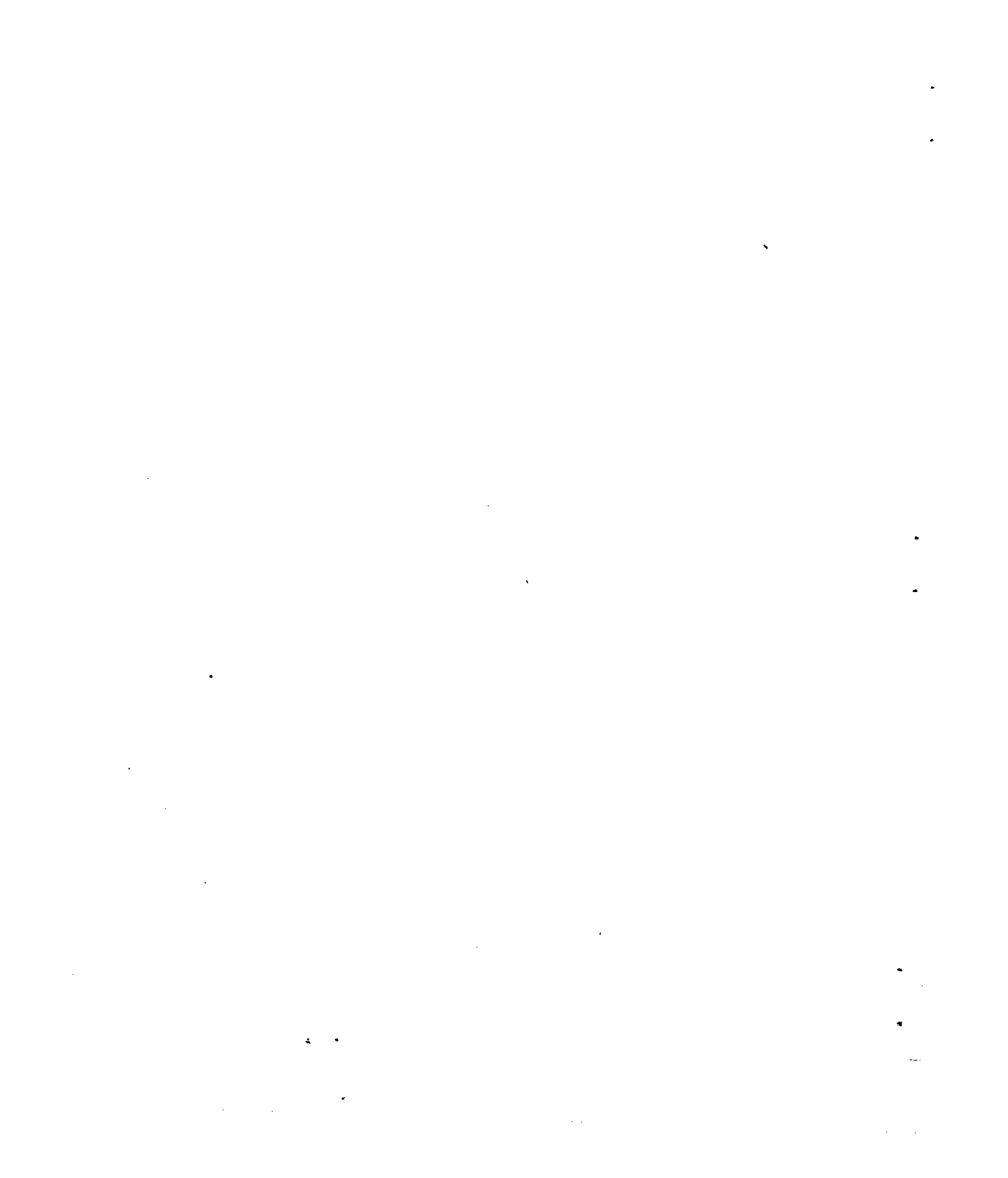
<sup>a</sup>Inspection was made with nozzle diaphragm in engine between runs; all other inspections were during overhaul periods.



TABLE III - NUMBER OF CRACKS IN NOZZLE BLADES AT CONCLUSION OF  
OPERATION AS DETERMINED BY FLOURESCENT-OIL INSPECTION

[Nozzle diaphragm 2 after 80 cycles (26 hr, 40 min) had only two cracks in leading edge and one crack in trailing edge of blade 4.]

Blade	Nozzle diaphragm 1 after 240 cycles (80 hr)		Nozzle diaphragm 3 after 319 cycles (106 hr, 20 min)	
	Edge		Edge	
	Leading	Trailing	Leading	Trailing
1	2	4	0	0
2	1	1	10	4
3	5	1	5	3
4	0	0	4	1
5	0	0	1	0
6	0	1	1	2
7	7	2	2	2
8	0	1	0	0
9	0	0	13	4
10	14	2	18	3
11	0	1	0	0
12	0	0	19	2
13	0	0	19	4
14	10	2	4	2
15	5	0	4	0
16	0	0	20	2
17	1	0	16	0
18	16	0	6	0
19	0	0	6	1
20	2	0	6	1
21	6	0	11	1
22	0	0	0	0
23	0	1	8	1
24	6	1	9	2
25	0	0	12	1
26	5	0	13	0
27	8	1	6	1
28	0	0	5	1
29	0	0	12	0
30	5	1	15	2
31	3	1	0	1
32	0	0	0	0
33	0	0	16	1
34	5	0	0	1
35	4	1	0	0
36	0	0	5	1
37	0	0	11	4
38	2	1	0	2
39	0	2	0	2
40	0	0	8	3
41	3	0	13	1
42	1	1	0	0
43	0	0	1	1
44	6	6	17	2
45	4	0	3	0
46	6	1	0	0
47	0	0	19	2
48	2	0	23	4



1212

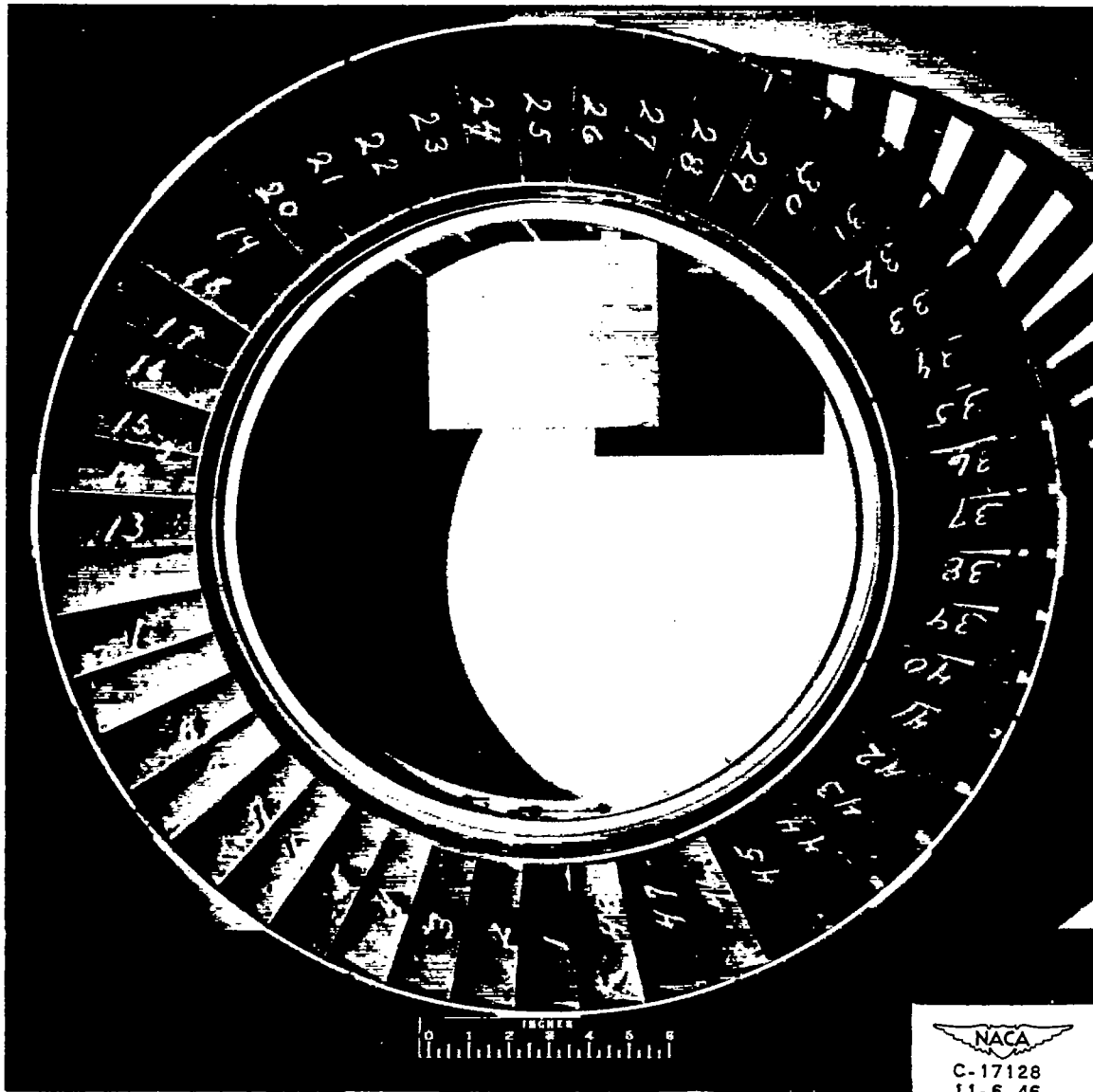
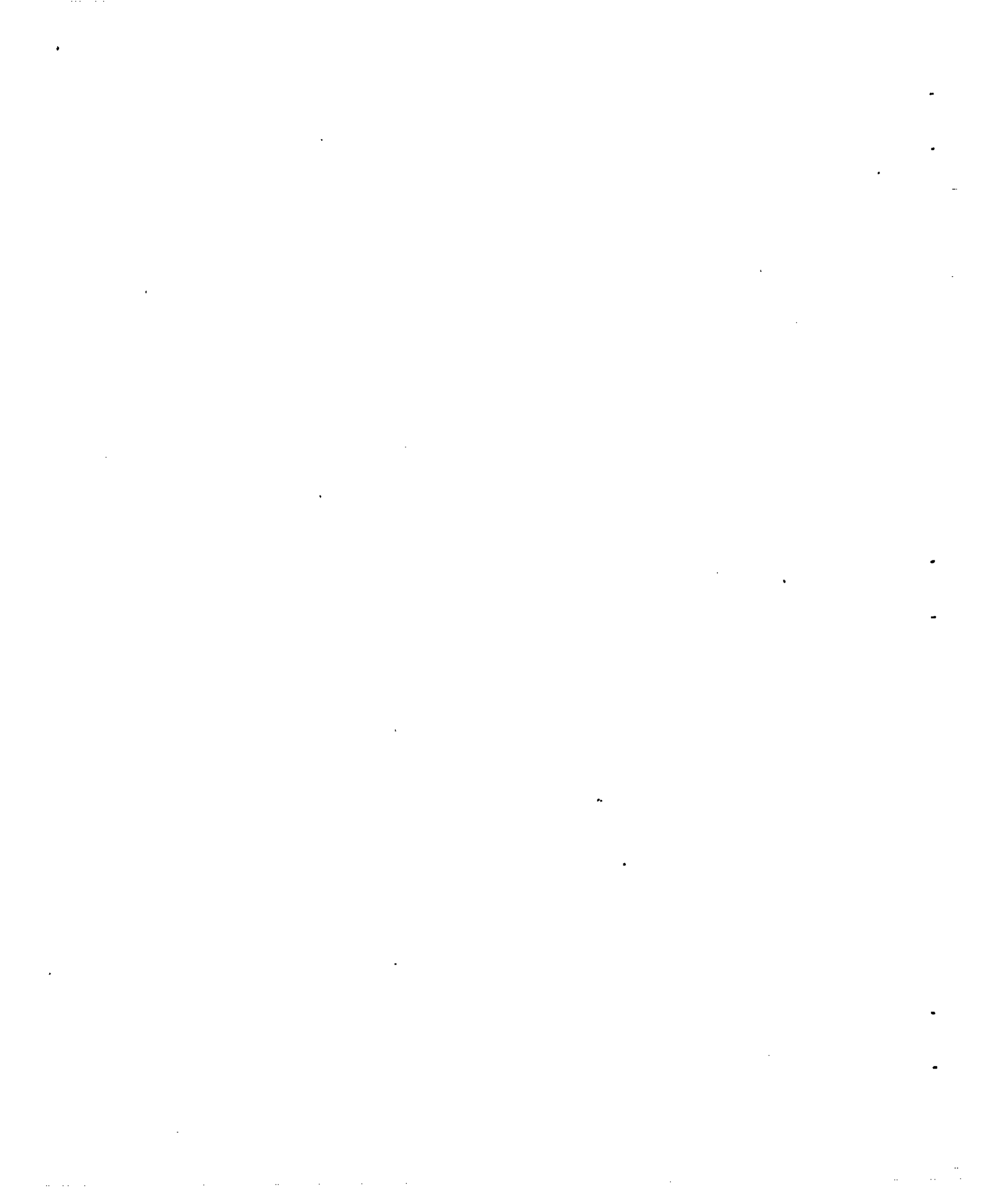
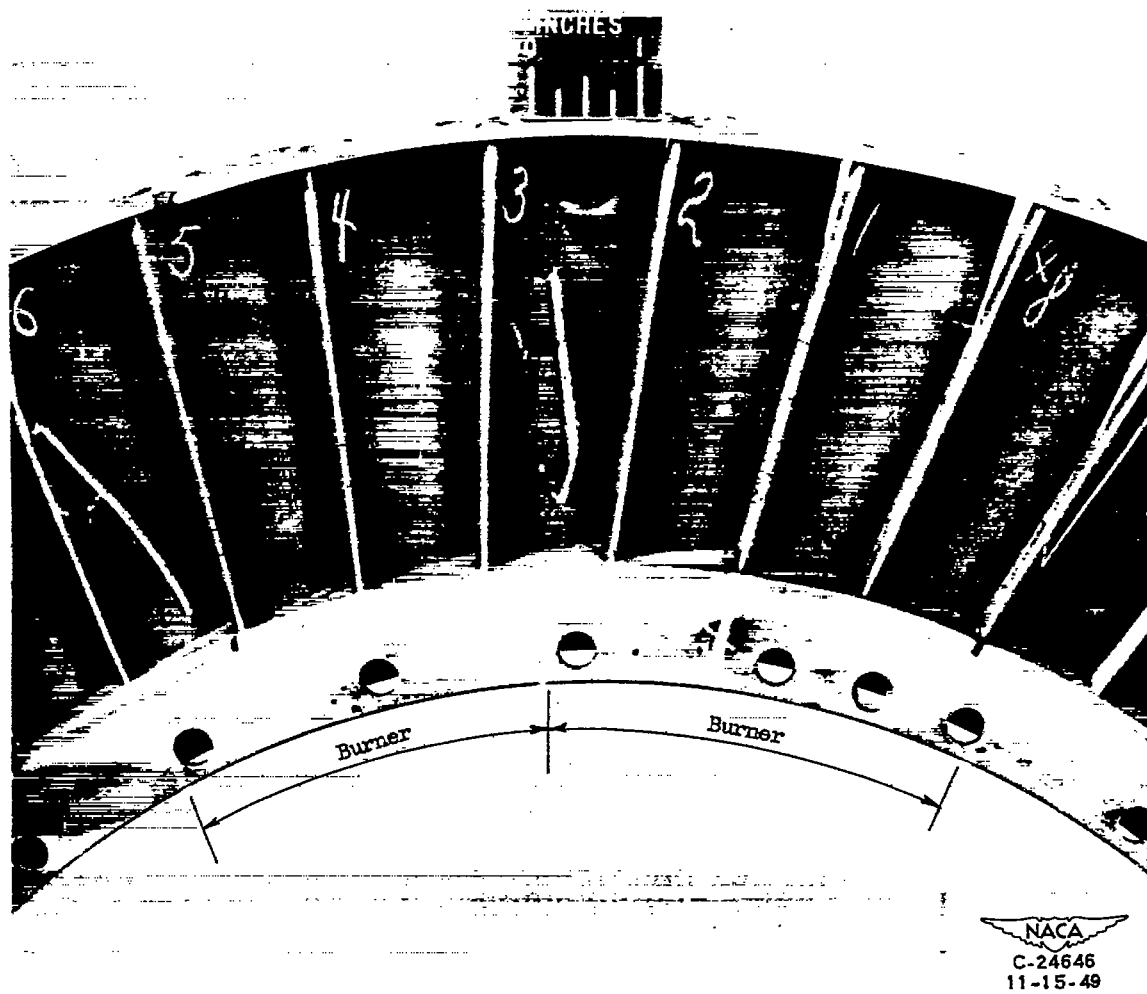


Figure 1. - Downstream face of nozzle diaphragm before engine operation.

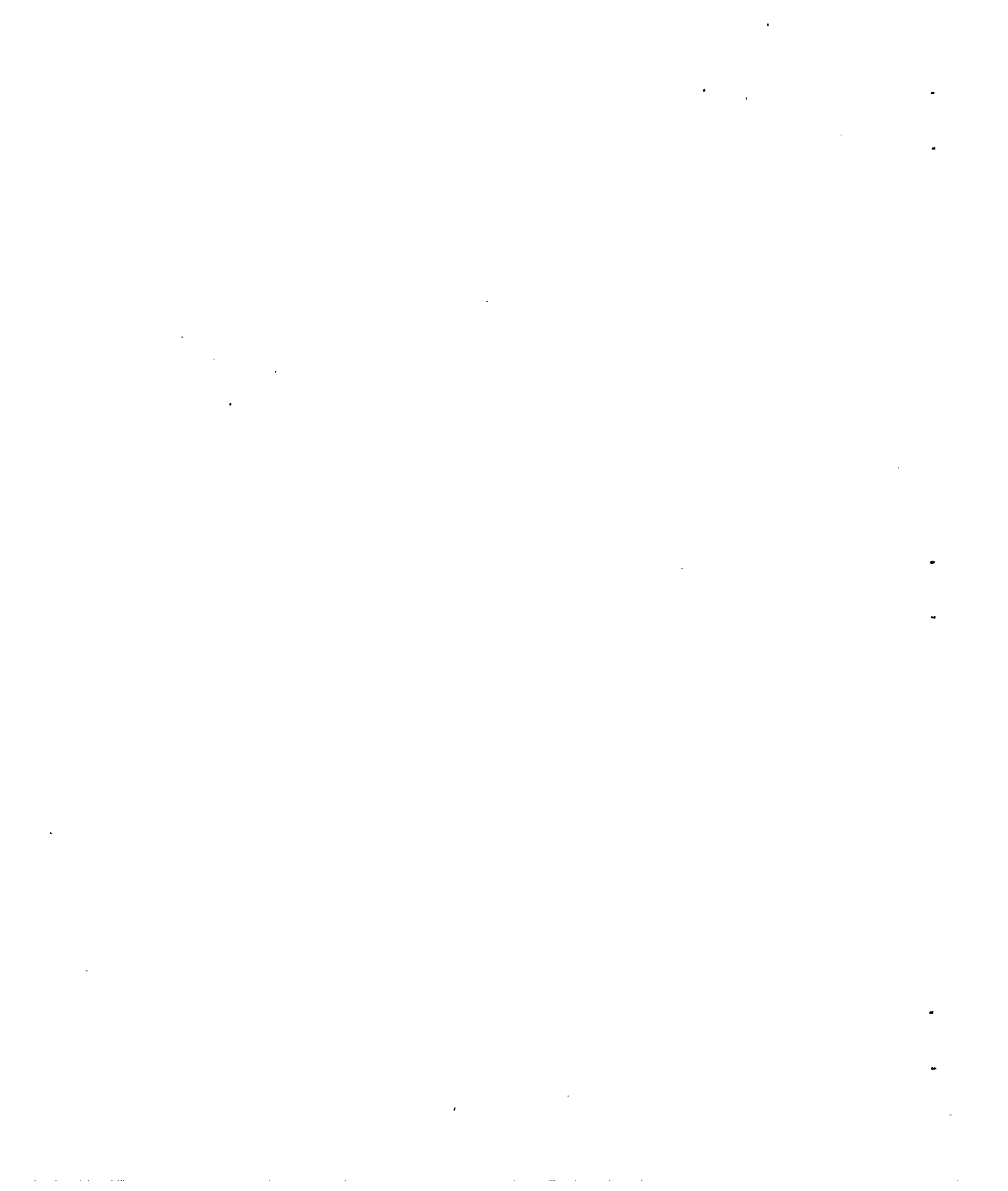


1212

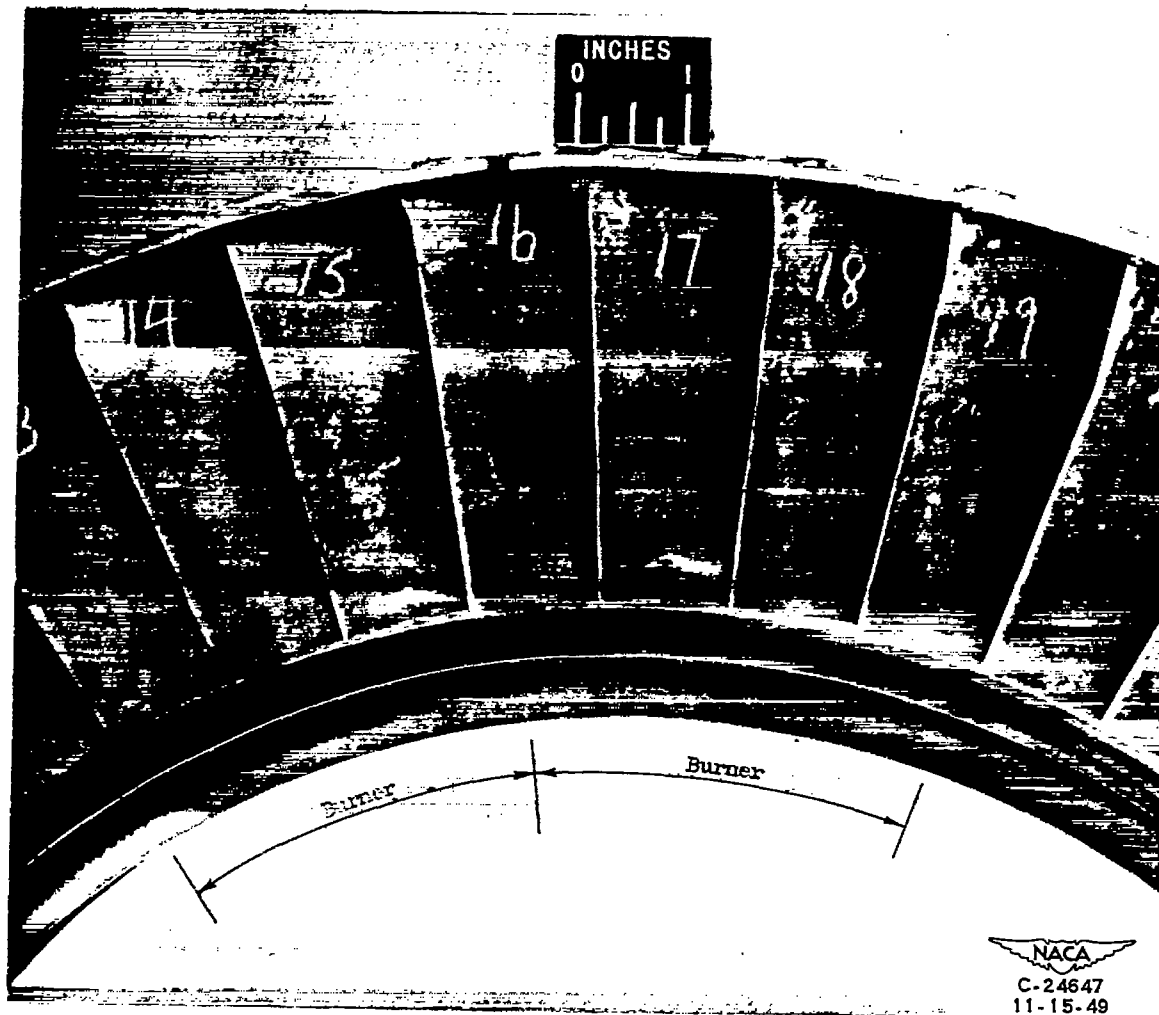


(a) Upstream face.

Figure 2. - Portion of nozzle diaphragm 3 after 319 cycles (106 hr, 20 min) showing blade condition with respect to burner locations.

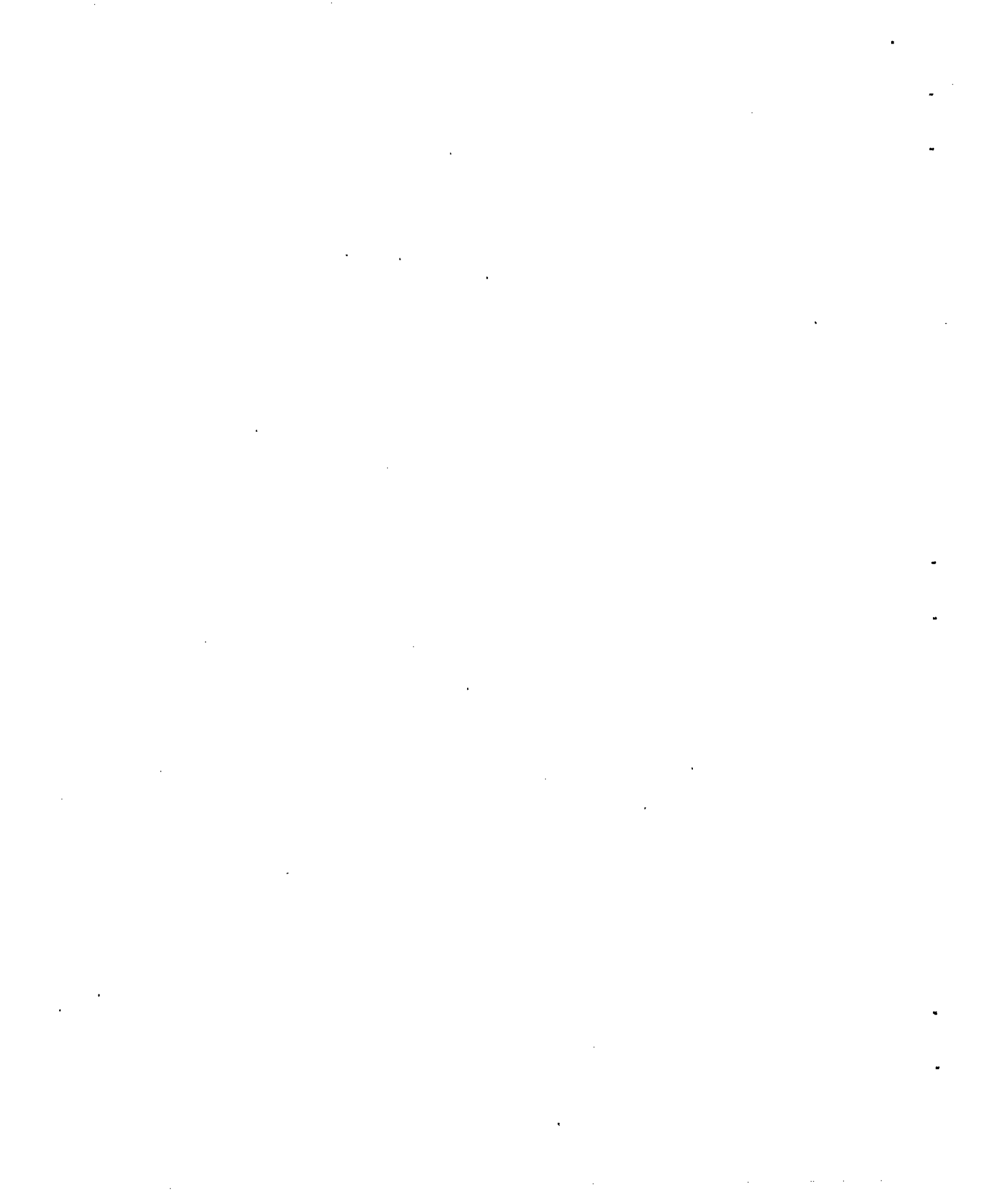


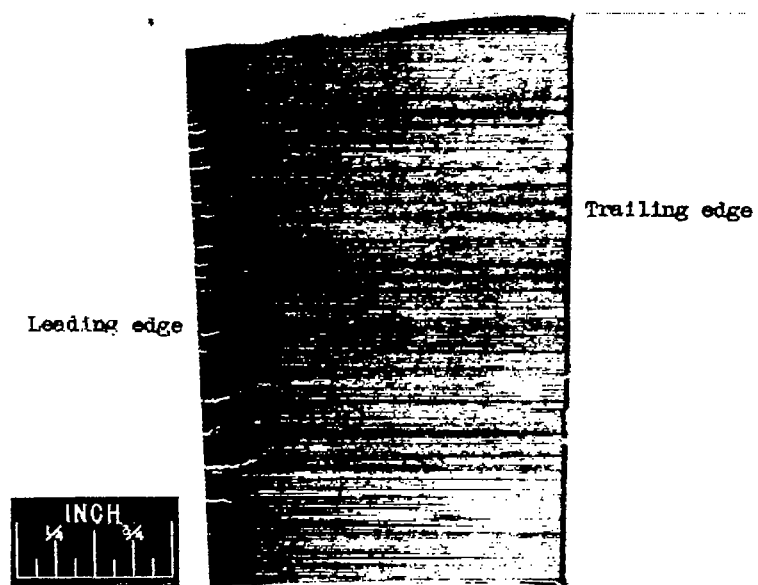
1212



(b) Downstream face.

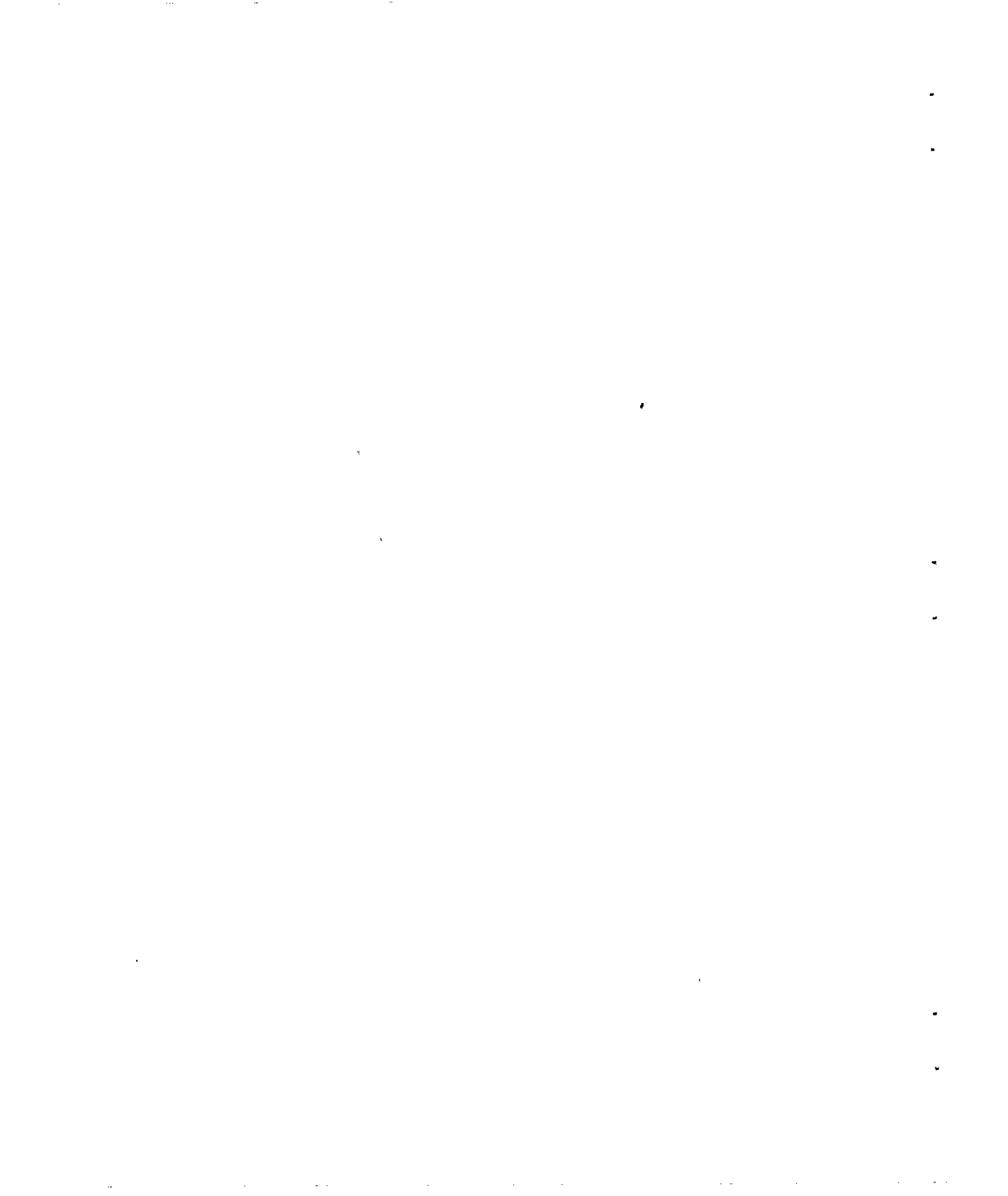
Figure 2. - Concluded. Portion of nozzle diaphragm 3 after 319 cycles (106 hr, 20 min) showing blade condition with respect to burner locations.





C-24648  
11-15-49

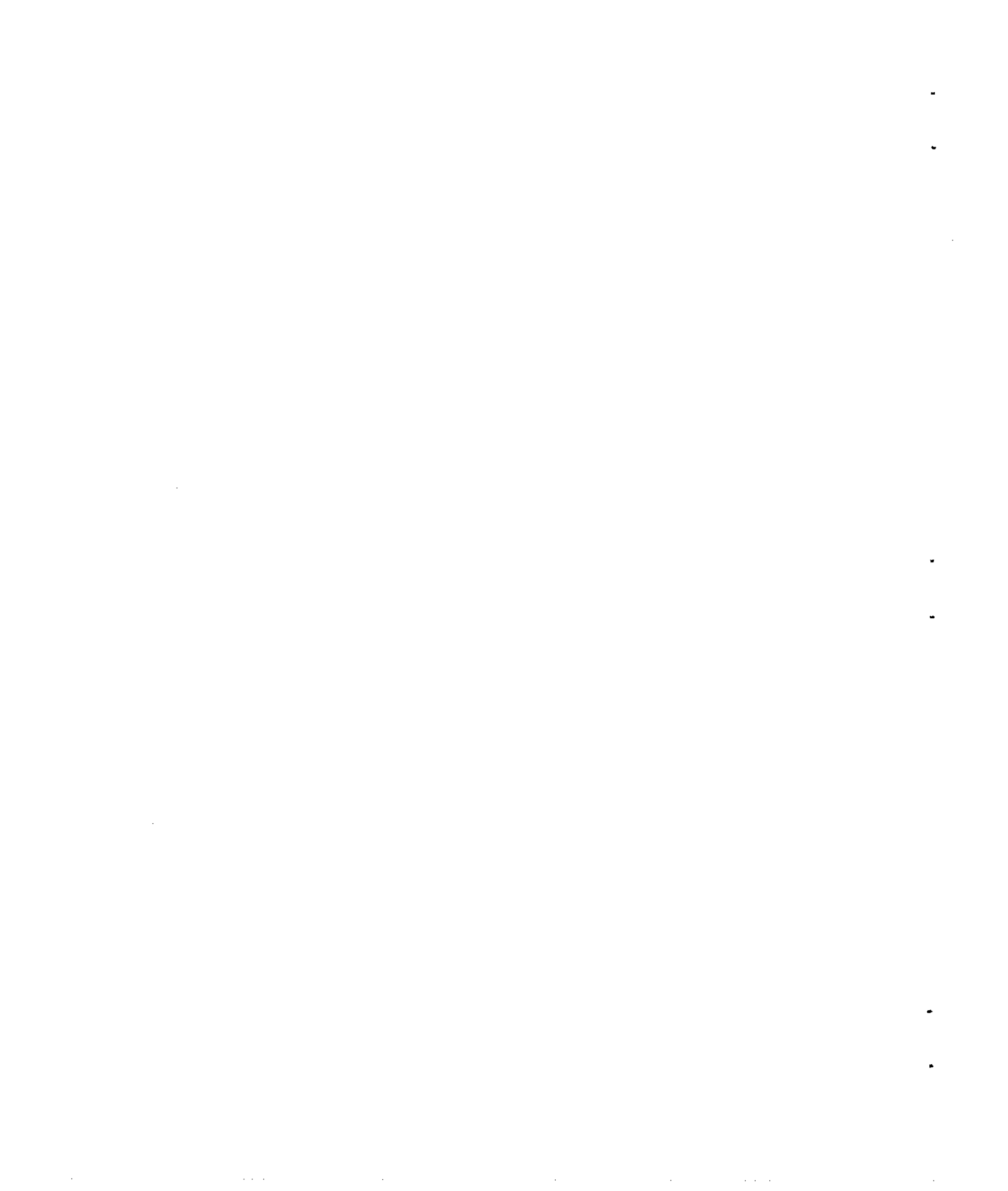
Figure 3. - Typical cracks in nozzle diaphragm blade after 319 cycles (106 hr, 20 min).





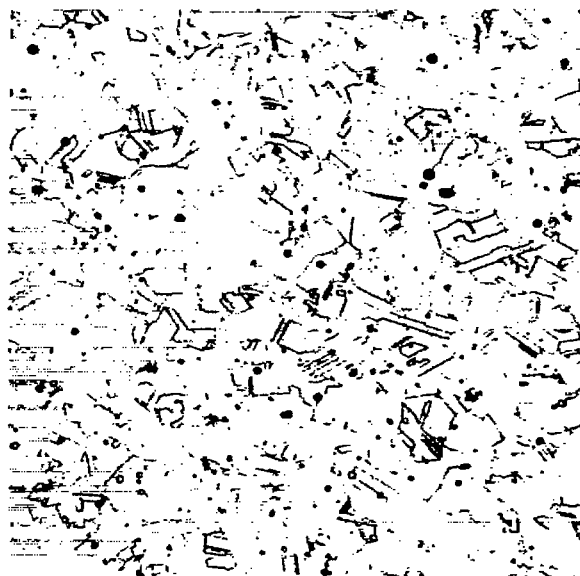
C-24649  
11-15-49

Figure 4. - Typical inner-spacer ring and weld cracks in nozzle diaphragm 3 after 319 cycles (106 hr, 20 min) of operation.





(a) AISI 321 stainless steel (titanium modified).

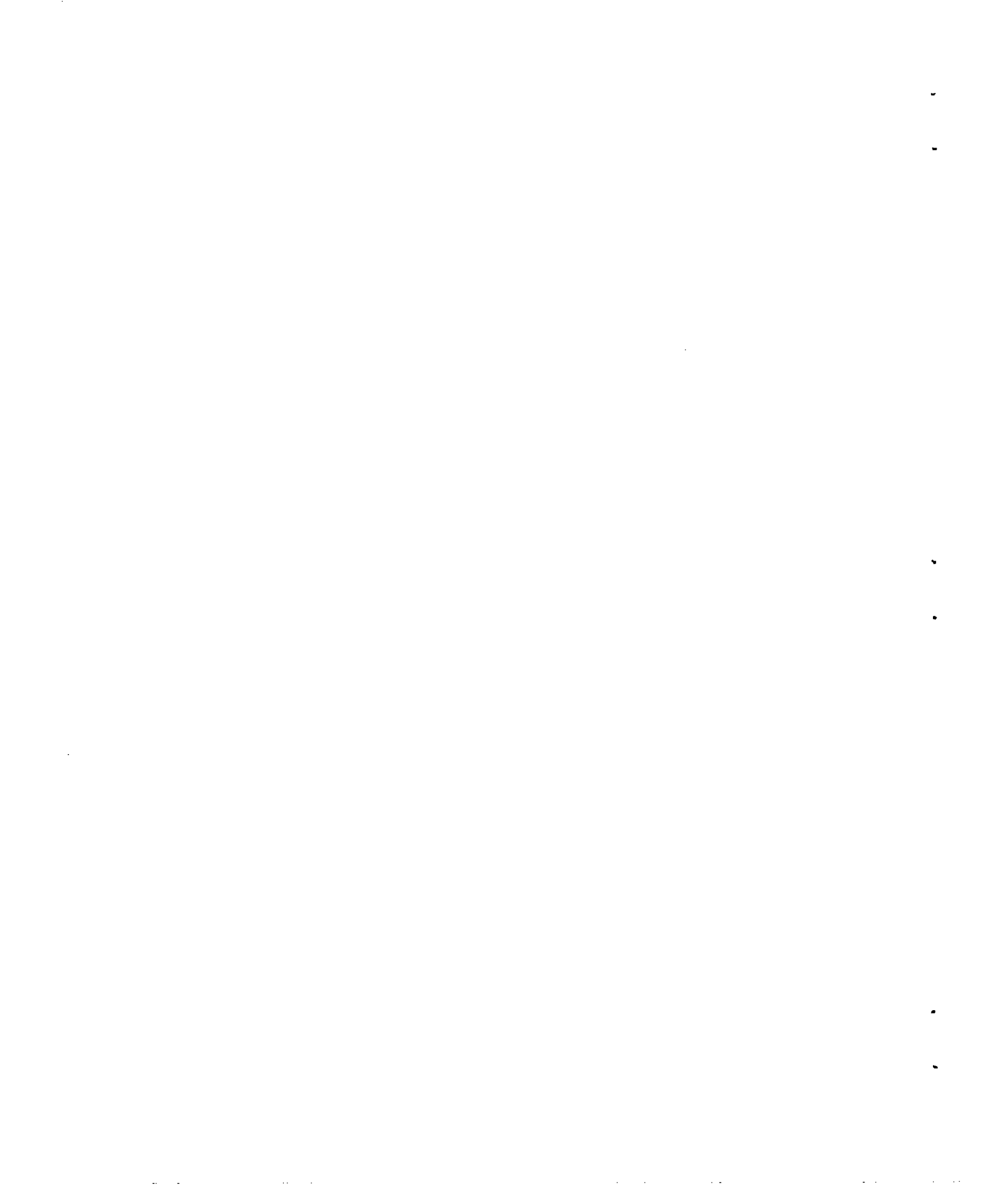


(b) AISI 347 stainless steel (columbium modified).

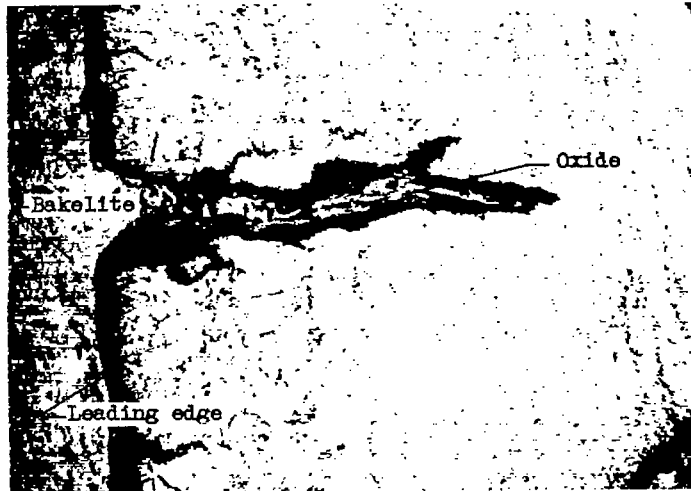
Figure 5. - Microstructure of nozzle blades before operation. X250.



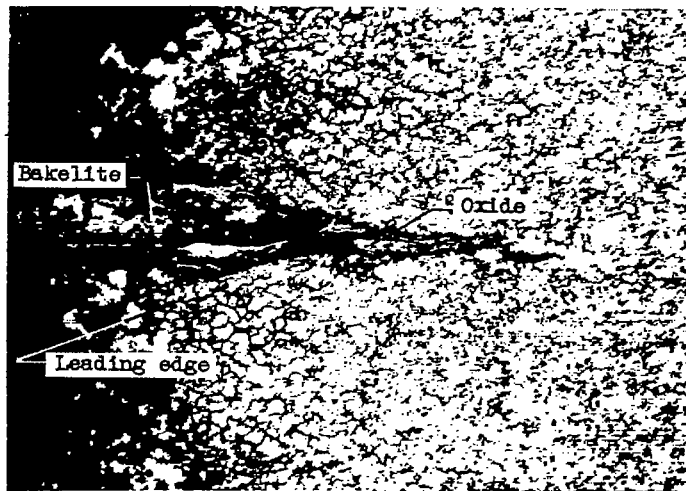
C-24650  
11-15-49



2121



(a) AISI 321 stainless steel (titanium modified).



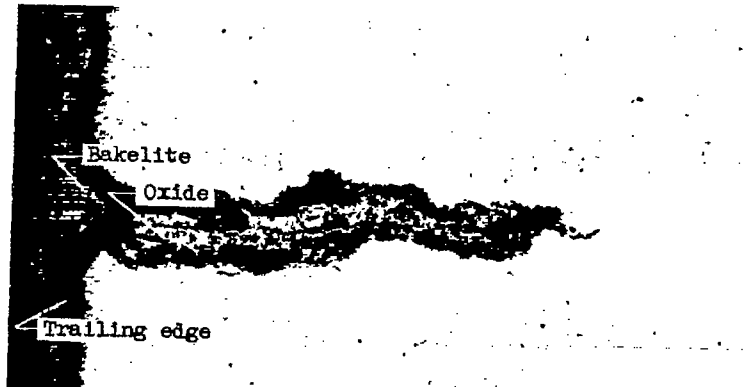
(b) AISI 347 stainless steel (columbium modified).

NACA  
C-24651  
11-15-49

Figure 6. - Typical leading-edge cracks after 319 cycles (106 hr, 20 min) of operation.  
X100.



1212



(a) Crack. X100



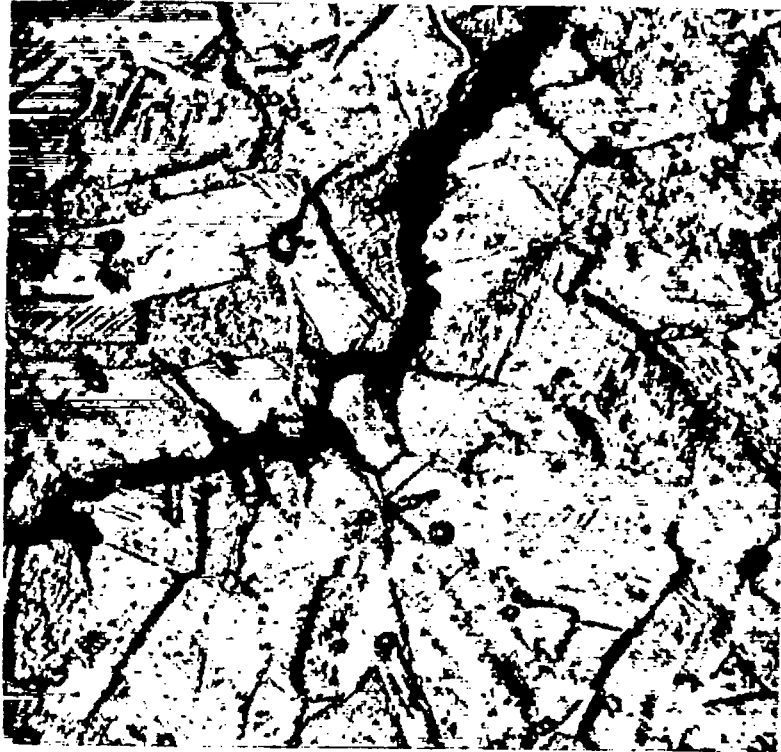
(b) Area alongside crack. X250

Figure 7. - Typical trailing-edge crack of AISI 347 stainless steel after 319 cycles (106 hr, 20 min) of operation.

NACA  
C-24652  
11-15-49



1212



NACA  
C-24653  
11-15-49

Figure 8. - Intergranular crack propagation in AISI 347 stainless steel after 80 cycles (26 hr, 40 min) of operation. Oblique illumination; X1000.

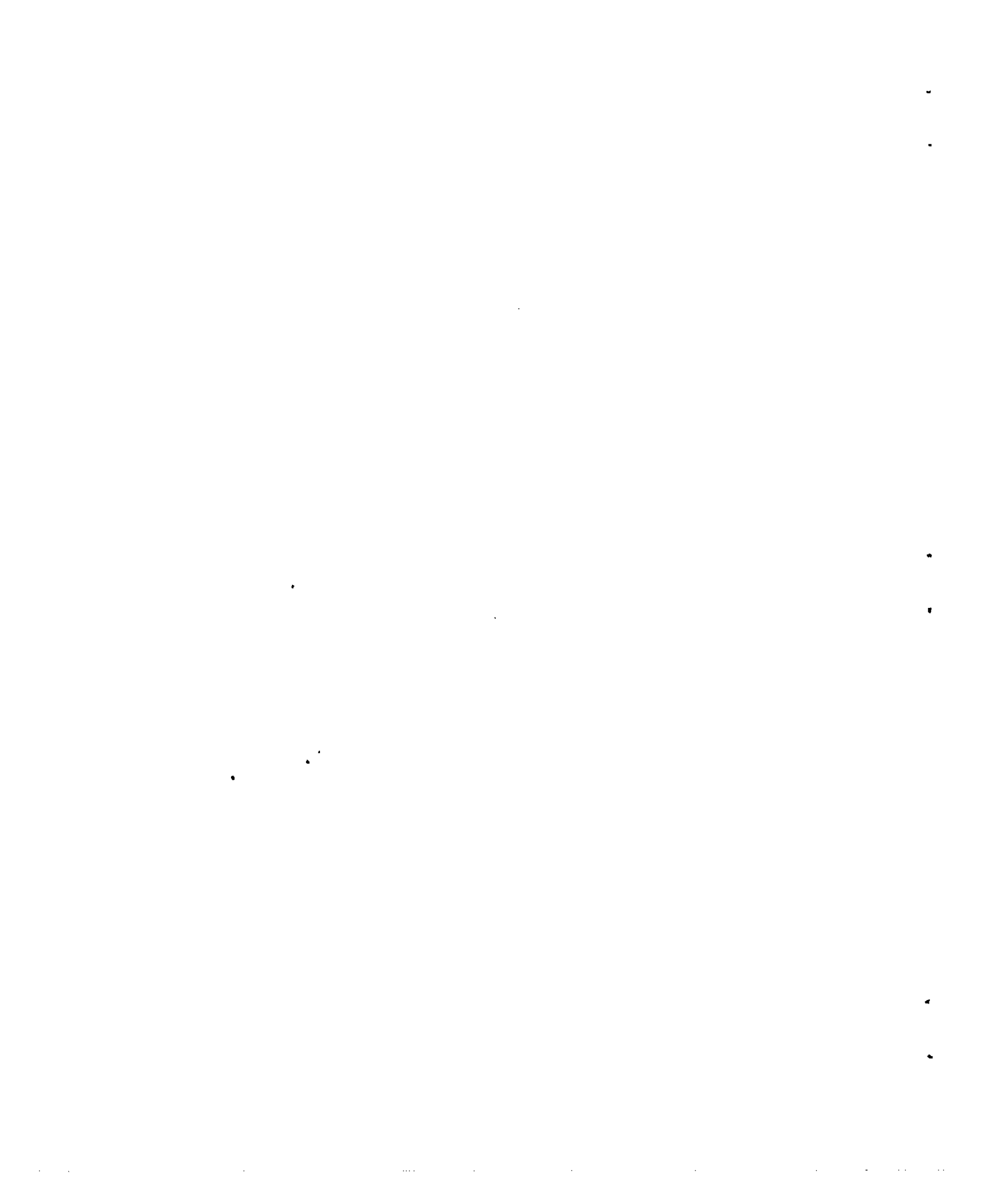


1212



NACA  
C-24654  
11-15-49

Figure 9. - Initial crack penetration in AISI 321 stainless steel after 319 cycles (106 hr, 20 min) of operation. X500.



1212

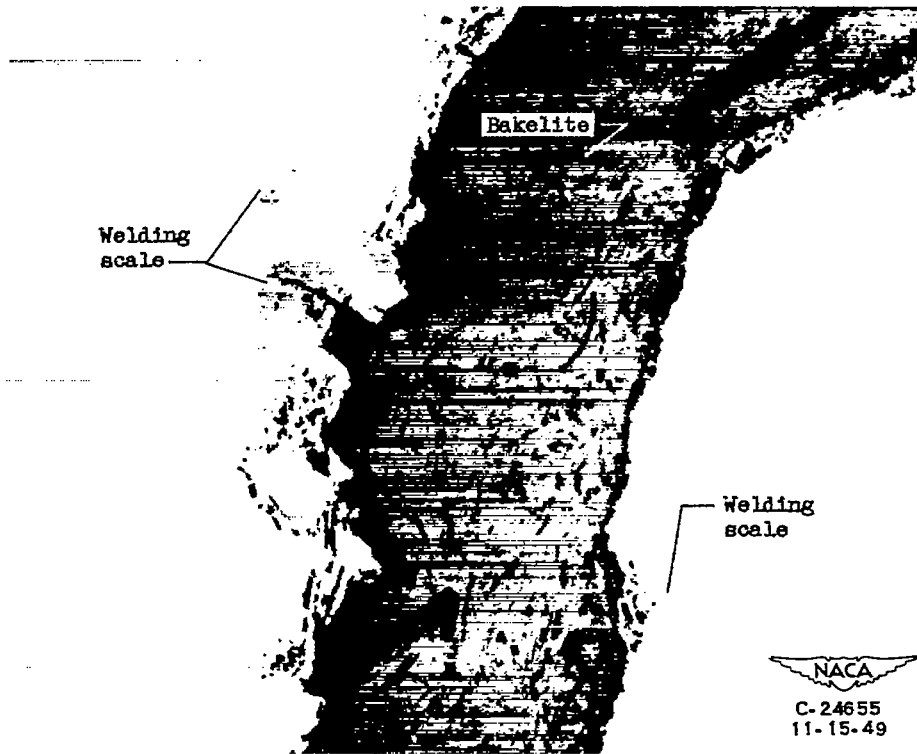


Figure 10. - Typical weld crack in AISI 347 stainless steel after 319 cycles (106 hr, 20 min) of operation. Unetched; X100.